

PREPARED FOR SUBMISSION TO JHEP

3.5-keV X-ray line from nearly-degenerate WIMP dark matter decays

Cheng-Wei Chiang^{a,b,c} and Toshifumi Yamada^a

^a*Department of Physics and Center for Mathematics and Theoretical Physics,
National Central University, Chungli, Taiwan 32001, Republic of China*

^b*Institute of Physics, Academia Sinica, Taipei, Taiwan 11529, Republic of China*

^c*Physics Division, National Center for Theoretical Sciences,
Hsinchu, Taiwan 30013, Republic of China*

ABSTRACT: The unidentified emission line at the energy of ~ 3.5 keV observed in X-rays from galaxy clusters may originate from a process involving a dark matter particle. On the other hand, a weakly interacting massive particle (WIMP) has been an attractive dark matter candidate, due to its well-understood thermal production mechanism and its connection to physics at the TeV scale. In this paper, we pursue the possibility that the 3.5-keV X-ray arises from a late time decay of a WIMP dark matter into another WIMP dark matter, both of which have the mass of $O(100)$ GeV and whose mass splitting is about 3.5 keV. We focus on the simplest case where there are two Majorana dark matter particles and two charged scalars that couple with a standard model matter particle. By assuming a hierarchical structure in the couplings of the two dark matter particles and two charged scalars, it is possible to explain the 3.5-keV line and realize the WIMP dark matter scenario at the same time. Since the effective coupling of the two different Majorana dark matter particles and one photon violates CP symmetry, the model always contains a new source of CP violation, so the model's connection to the physics of electric dipole moments is discussed. The model's peculiar signatures at the LHC are also studied. We show the prospect of detecting the charged scalars through a detailed collider simulation.

Contents

1	Introduction	1
2	The Model	4
3	Relic Abundance	5
4	Dark Matter Decay Rate	7
5	Numerical Analysis on the Coupling Constants	9
6	Phenomenology	10
6.1	Electric Dipole Moments	10
6.2	Signatures at the LHC	11
7	Summary	14

1 Introduction

Although existence of dark matter (DM) is firmly believed through observations of its gravitational effects, its detailed properties and interactions with the visible sector other than gravity remain largely unknown. Recently, a faint hint on the nature of DM has been reported by two groups [1, 2] through observations of the X-ray spectrum from galaxy clusters. They claim that they have discovered a weak X-ray emission line at the energy of about 3.5 keV that cannot be explained by any known atomic electron transition in thermal plasma, and that this line is possibly due to the decay of a DM particle, with one example being the decay of a 7 keV sterile neutrino into a photon and an active neutrino. If the emission line originates from a DM particle, we then have an important clue on possible interactions of the DM; namely, this particle couples with the photon in such a way that its interaction involves a 3.5-keV monochromatic photon. Many studies have been done on the connection between the DM physics and the 3.5-keV X-ray line [3].

On the other hand, there has been another hint on the nature of DM from theoretical studies; that is, the so-called weakly interacting massive particle (WIMP) miracle. If the DM particle that is responsible for the observed DM abundance couples with a standard model (SM) particle through a coupling constant of order 0.1, and if it is a cold relic of thermal plasma in the early Universe (these are the case when the DM particle is a WIMP), then its interaction with the SM sector

should involve a particle of $O(100)$ GeV mass, just above the electroweak symmetry breaking scale where new physics is expected to enter. In addition, if the DM particle has the same new physics origin as the new particle that mediates the interaction between the DM sector and the SM sector, then it is natural to consider that the DM particle itself has the mass of $O(100)$ GeV.

In this paper, we propose a scenario that accommodates both the hint of DM that may be responsible for the 3.5-keV X-ray emission line and the scenario of WIMPs with mass of $O(100)$ GeV. In the scenario, there are two species of WIMP DM particles whose masses are both $O(100)$ GeV and whose mass difference is about 3.5 keV. Both DM species are stable at the cosmological time scale. The heavier DM particle decays into the lighter one and a 3.5-keV photon with a rate below $\sim 1/t_{cos}$, where t_{cos} denotes the age of the Universe, giving rise to the observed monochromatic 3.5-keV X-ray emission line.

Let us now determine the structure of one of the simplest models. First, we discuss in what cases the decay of a DM particle into another DM particle and a photon is realized. Scalar DM particles are impossible because the decay of a scalar particle into another scalar particle and a photon is forbidden by angular momentum conservation. Hence the next possibility is the case with spin-1/2 Majorana fermions. Majorana particles interact with an *on-shell* photon *only* through the following dipole transition operators [4], where χ_1 and χ_2 are different mass eigenstates:

$$\frac{1}{\Lambda} \bar{\chi}_2 \sigma_{\mu\nu} \chi_1 F^{\mu\nu}, \quad \frac{1}{\Lambda} \bar{\chi}_2 \sigma_{\mu\nu} \gamma_5 \chi_1 F^{\mu\nu}. \quad (1.1)$$

In fact, it is known that spin-1/2 particles can interact with a photon also through an anapole coupling [5]. But this coupling vanishes identically when the photon is on shell.

Next, we pin down the structure of the interaction between our Majorana DM particles and SM particles that allows the DM particles to be the WIMPs. If the DM particles interact with the SM sector only through the operators in Eq. (1.1) with $\mathcal{O}(1)$ coefficients, then WIMP miracle would suggest that $\Lambda = O(100) - O(1000)$ GeV. However, this would give too large a decay rate for the heavier DM particle, far above the inverse of the age of the Universe, leading to the situation where the abundance of the heavier DM at present is extremely suppressed and the photon flux coming from its decay is insufficient to explain the observed 3.5-keV X-ray line. One simple solution to this difficulty is to consider the following renormalizable interaction Hamiltonian which induces the interactions in Eq. (1.1) at one-loop level,

$$\mathcal{H}_{\text{int}} = \lambda_{ij}^L \bar{\chi}_i P_L \psi S_j + \lambda_{ij}^R \bar{\chi}_i P_R \psi S_j + \text{h.c.} \quad (i, j = 1, 2), \quad (1.2)$$

where S_1, S_2 denote two scalar fields and ψ denotes a spin-1/2 field, both of which have electric charges, and the coupling constants $\lambda_{11}, \lambda_{22}$ are assumed to be of $O(0.1)$

whereas $\lambda_{12}, \lambda_{21}$ are much more suppressed. In the following, we assume that the decays of $\chi_i \rightarrow \psi S_j$ are kinematically forbidden for the stability of the DM particles.

The right thermal relic abundance of DM particles can be achieved in the following two scenarios. In the first scenario, ψ is lighter than χ_i s and S_i s have the mass of $O(100)$ GeV. In this case, ψ is in thermal equilibrium with SM particles through the electroweak interactions when χ_i s go out of thermal equilibrium. The fact that $\lambda_{11}, \lambda_{22}$ are $O(0.1)$ and S_i s have the mass of $O(100)$ GeV guarantees that the thermal relic abundance of χ_i s fits the observed DM abundance $\Omega_{DM} h^2 \sim 0.1$. The other possibility is that S_i s are lighter than χ_i s and ψ has the mass of $O(100)$ GeV, in which case the thermal relic abundance of χ_i s again can fit the observed DM abundance. To avoid the presence of a stable charged particle, ψ (if ψ is lighter than the DMs) or S_i s (if S_i s are lighter than the DMs) should be or eventually decay into SM particles. We shall adopt the simplest case in which ψ is lighter than the DM particles and is identified as a SM matter field with an electric charge.

On the other hand, the decay rate of the heavier DM species into the lighter one and the photon is controlled by the coupling constants λ_{12} and λ_{21} , and hence the photon flux of the 3.5-keV X-ray line can be explained by taking appropriate values for these constants.

To summarize, the simplest model that can explain the 3.5-keV X-ray line by a WIMP DM decay into another WIMP DM and a photon has two species of spin-1/2 Majorana DM particles that couple with two charged scalar particles of $O(100)$ GeV mass and an electrically-charged SM particle. The coupling constants for the DM particles have a hierarchical structure that each DM particle dominantly couples with a distinct charged scalar with the strength of $O(0.1)$, and couples with the other charged scalar with a much more suppressed strength. The $O(0.1)$ coupling constants are responsible for obtaining the right thermal relic abundance of DM particles, as they control the decoupling of DM particles from the thermal bath in the early Universe. On the other hand, the suppressed coupling constants are responsible for reproducing the observed photon flux of the 3.5-keV X-ray line, as they determine the decay rate of the heavier DM species into the lighter one and the photon. Phenomenologically important is the fact that the combination of the WIMP DM scenario and the 3.5-keV X-ray line predicts, in the simplest case, the existence of *two* charged scalars that couple with the DM particles and a SM matter field, which is testable in collider experiments.

In this paper, we construct a concrete WIMP DM model based on the above arguments, and derive the coupling constants λ_{ij} s that reproduce the observed flux of the 3.5-keV X-ray line and the right thermal relic abundance of DM. We concentrate on the simplest case where, among the SM matter fields, an $SU(2)_L$ -singlet charged lepton couples with the DMs and the charged scalars. Extensions to cases where other SM matter fields couple with the DMs and the charged scalars are straightforward.

This paper is organized as follows. In section 2, we describe our DM model by

introducing the new particles, a pair of DM particles and a pair of charged scalars, as well as their interactions with one SM lepton, from which we derive the required magnetic dipole operator for the 3.5-keV X-ray line from DM decays. In section 3, we calculate the thermal relic density of the DM particles, from which correlation between the new interaction strength and the DM mass is obtained. Section 4 concerns with the decay rate of the heavier DM particle to the lighter one and the 3.5-keV photon, which demands CP-violating couplings in the new interactions. Combining the current data of the DM relic abundance and the 3.5-keV X-ray line, we perform a numerical analysis to find viable parameter regions in our model. In section 6, we evaluate the electric dipole moment of the SM lepton that couples with the DM particles, and perform a collider simulation for the signature of charged scalar pair production at the 14-TeV LHC. Section 7 summarizes our findings.

2 The Model

We introduce two spin-1/2 Majorana fields χ_1, χ_2 , which are neutral under the SM gauge groups, and two scalar fields S_1, S_2 with hypercharge $Y = +1$ but otherwise neutral under $SU(3)_C$ and $SU(2)_L$. A Z_2 symmetry is imposed, under which χ_i, S_i ($i = 1, 2$) are odd and the SM fields are even.¹ χ_i and S_i are the mass eigenstates with eigenvalues m_i and M_i ($i = 1, 2$), respectively. The masses m_1, m_2 and M_1, M_2 are of $O(100)$ GeV, with m_1, m_2 being smaller than M_1, M_2 . Both χ_1, χ_2 are assumed to be stable at the scale of the age of the Universe ($t \simeq 4.4 \times 10^{17}$ s) and constitute the DM of the Universe. It is further assumed that m_2 is larger than m_1 by about 3.5 keV, and that χ_2 decays into χ_1 and a 3.5-keV photon at a rate below the inverse of the age of the Universe, giving rise to the observed 3.5-keV monochromatic photon flux. Hence the masses of χ_1 and χ_2 are highly degenerate with a fine-tuning of order $\sim 3.5 \text{ keV}/100 \text{ GeV} \sim 10^{-8}$. We shall leave the issue of naturally explaining this mass degeneracy for future studies, and regard the degeneracy as a working assumption of the model.

The interaction Hamiltonian involving the fields χ_i and S_i is given by

$$\mathcal{H}_{\text{int}} = \lambda_{ij} \bar{\chi}_i \ell_R S_j + \text{h.c.}, \quad (i, j = 1, 2) \quad (2.1)$$

where ℓ_R denotes a SM $SU(2)_L$ -singlet charged lepton, and repeated indices are understood to be summed over. It could be the case that χ_i and S_i ($i = 1, 2$) couple with charged leptons of different flavors. However, this would give rise to lepton flavor-violating processes that are under severe experimental constraints. To evade such constraints and for simplicity, we assume that χ_i and S_i ($i = 1, 2$) couple with only one SM lepton. We note that the diagonal couplings λ_{11} and λ_{22} can be made

¹ This Z_2 symmetry may be the remnant of a new $U(1)_X$ gauge symmetry under which χ_i, S_i are oddly charged while all the SM fields are evenly charged.

real and positive by rotating the phases of S_i , whereas the off-diagonal couplings λ_{12} and λ_{21} are generally complex and can potentially lead to CP-violating phenomena for the SM lepton.

The DM particles χ_1, χ_2 interact with the SM sector through the interactions in Eq. (2.1). With appropriate choices of the interaction strengths, the thermal relic abundance of χ_1 and χ_2 can fit the observed DM abundance.

At one-loop level, the following effective interaction is induced:

$$\mathcal{H}_{eff} = C \bar{\chi}_1 \sigma_{\mu\nu} \chi_2 F^{\mu\nu} , \quad (2.2)$$

where the coefficient C can be expressed in terms of the coupling constants λ_{ij} and mass eigenvalues m_i, M_i ($i, j = 1, 2$) when the SM lepton mass is neglected. The interaction in Eq. (2.2) gives rise to the decay process $\chi_2 \rightarrow \chi_1 \gamma$ that can explain the observed 3.5-keV X-ray line. We note in passing that the transition electric dipole coupling is not induced in our model because only one chirality of the charged lepton is involved.

In our model, the Majorana DM particles contribute to the spin-independent cross section for DM-nucleon elastic scattering only through the transition magnetic dipole coupling Eq. (2.2). However, the effective coupling of Eq. (2.2) should be extremely small to explain the 3.5-keV X-ray line. Therefore, the contribution to the spin-independent cross section is suppressed, and we are allowed to neglect the experimental bounds from DM direct detection experiments.

3 Relic Abundance

At high temperatures in the early Universe, the DM particles χ_1, χ_2 are in thermal equilibrium with the SM particles through the following processes with t -channel exchanges of the charged scalars S_1, S_2 :

$$\chi_1 \chi_1 \leftrightarrow \ell \bar{\ell} , \quad \chi_2 \chi_2 \leftrightarrow \ell \bar{\ell} . \quad (3.1)$$

Processes involving both χ_1 and χ_2 are negligibly rare, because the coupling constants λ_{12} and λ_{21} must be extremely suppressed in order to explain the 3.5-keV X-ray line observed today. Below the temperature of $T_{dec} \sim m_1/20 \simeq m_2/20$, the DM particles decouple from the thermal bath and their abundance freezes out.

The squared amplitude for the process $\chi_i \chi_i \leftrightarrow \ell \bar{\ell}$ ($i = 1, 2$) with spin summations

over *initial* and final state particles is given by [6]

$$|\mathcal{M}_i(s)|^2 = \frac{|\lambda_{ii}|^4}{16\pi} 4 \left[(M_i^2 - m_i^2)^2 + \frac{s}{2} m_i^2 \right] \times \frac{\frac{s}{2} \sqrt{1 - \frac{4m_i^2}{s}} \left(\frac{s}{2} - m_i^2 + M_i^2 \right) - \{ (M_i^2 - m_i^2)^2 + s M_i^2 \} \tan^{-1} \left(\frac{s/2 \sqrt{1 - 4m_i^2/s}}{s/2 - m_i^2 + M_i^2} \right)}{\frac{s}{4} \sqrt{1 - \frac{4m_i^2}{s}} \left(\frac{s}{2} - m_i^2 + M_i^2 \right) \{ (M_i^2 - m_i^2)^2 + s M_i^2 \}}, \quad (3.2)$$

where $s = (p_1 + p_2)^2$ with $p_{1,2}$ being the 4-momenta of the initial-state particles. Assuming that the SM lepton ℓ remains in thermal equilibrium and neglecting its mass, the thermally-averaged rate of the pair-annihilation process $\chi_i \chi_i \rightarrow \ell \bar{\ell}$ ($i = 1, 2$) per pair of χ_i particles at temperature T is given by [8]

$$\langle \sigma v_i \rangle_T = \frac{1}{(n_{\chi_i}^{\text{eq}}(z))^2} \frac{T}{32\pi^4} \int_{4m_i^2}^{\infty} ds \sqrt{\frac{s}{4} - m_i^2} K_1 \left(\frac{\sqrt{s}}{T} \right) |\mathcal{M}_i(s)|^2, \quad (3.3)$$

where $n_{\chi_i}^{\text{eq}}$ is the density of the DM particle χ_i in thermal equilibrium,

$$n_{\chi_i}^{\text{eq}} = g_{\chi} \int \frac{d^3 \vec{p}}{(2\pi)^3} e^{-\sqrt{|\vec{p}|^2 + m_i^2}/T} \quad (3.4)$$

with $g_{\chi} = 2$ being the number of degrees of freedom for χ_1 or χ_2 , and $K_1(x)$ is the modified Bessel function of the second kind of order 1.

We apply an approximation formula given in Ref. [7] to estimate the relic abundance of χ_1 and χ_2 . To use the formula, we note that $\langle \sigma v_i \rangle_T$ can be approximated for $m_i/T \gtrsim 3$ as

$$\langle \sigma v_i \rangle_T \simeq |\lambda_{ii}|^4 \sigma_{i0}(M_i) \left(\frac{m_i}{T} \right)^{-3}, \quad (3.5)$$

where σ_{i0} depends only on M_i . Then the mass density of the DM particle χ_i ($i = 1, 2$) is given by

$$\Omega_{\chi_i} h^2 \simeq 1.07 \times 10^9 \frac{(n+1)x_f^{n+1}}{(g_{*S}/\sqrt{g_*}) M_{Pl} |\lambda_{ii}|^4 \sigma_{i0}} \text{ GeV}, \quad (3.6)$$

where x_f^i corresponds to an estimated decoupling temperature as $x_f^i = m_i/T_{\text{dec}}$ and is given by

$$x_f^i \simeq \log[0.038(n+1)(g_{\chi}/\sqrt{g_*}) M_{Pl} m_i |\lambda_{ii}|^4 \sigma_{i0}] - \left(n + \frac{1}{2} \right) \log[\log[0.038(n+1)(g_{\chi}/\sqrt{g_*}) M_{Pl} m_i |\lambda_{ii}|^4 \sigma_{i0}]], \quad (3.7)$$

with $n = 3$ here, M_{Pl} is the Planck mass, and $g_*, g_{*S} = 86.25$ are respectively the numbers of relativistic degrees of freedom for the energy density and entropy density

at about the decoupling temperature $T_{dec} \sim m_i/20 \sim O(10)$ GeV. Even though χ_2 eventually decays into χ_1 , the net mass density of χ_1 and χ_2 is almost invariant throughout the evolution of the Universe as their mass difference is negligibly small compared to their masses.

Recently, the Planck Collaboration [9] reported the following DM mass density:

$$\Omega_{DM} h^2 = 0.1199 \pm 0.0027. \quad (3.8)$$

For given values of m_1, m_2 and M_1, M_2 , one can obtain information on the values of $\lambda_{11}, \lambda_{22}$ from Eq. (3.6) and the relation

$$\Omega_{\chi_1} h^2 + \Omega_{\chi_2} h^2 = \Omega_{DM} h^2. \quad (3.9)$$

For example, if the DM mass is given by $m_1 \simeq m_2 = 300$ GeV and the charged scalar mass by $M_1 \simeq M_2 = 400$ GeV, then the right thermal relic abundance of DM can be reproduced with the coupling constants of $\lambda_{11} = \lambda_{22} \simeq 0.5$.

4 Dark Matter Decay Rate

The heavier DM particle χ_2 decays into the lighter one χ_1 and the photon through the effective interaction in Eq. (2.2) induced at one-loop level. By assuming negligible mass difference between M_1 and M_2 and that between m_1 and m_2 when allowed, and defining $M \equiv M_1 \simeq M_2$, $m \equiv m_1 \simeq m_2$, we obtain the following decay rate of χ_2 :

$$\Gamma_{\chi_2} = \frac{k^3}{\pi} \left(\frac{1}{32\pi^2} \frac{m}{M^2} \frac{x + \log(1-x)}{2x^2} \right)^2 Q^2 \text{Im}(\lambda_{11}\lambda_{21}^* + \lambda_{12}\lambda_{22}^*)^2 \quad (4.1)$$

where k denotes the energy of the photon and is given by $k = m_2 - m_1 = 3.5$ keV. Q denotes the electric charge of the lepton, $Q = -e$, and x is defined as $x \equiv m^2/M^2$.²

Based upon the assumption that the observed 3.5-keV X-ray line originates from the decay of a sterile neutrino, Refs. [1, 2] have derived the mixing angle of the sterile neutrino with a SM active neutrino. Since the ratio of the DM decay rate over the DM mass appearing in the above calculation is a model-independent quantity, we are allowed to exploit that ratio for our model. According to Ref. [1], the ratio in our model assumes the following central value:

$$\frac{\Gamma_{\chi_2}}{m} = 2.4 \times 10^{-29} \text{ s}^{-1} \text{ keV}^{-1}. \quad (4.2)$$

On applying the result in Eq. (4.2) to our model, we should take into account the decrease in the number of χ_2 due to its decay, as the lifetime of χ_2 may not be much

² χ_2 can also decay into a χ_1 and two neutrinos. However, since an off-shell Z boson is involved, the partial width is negligibly small compared to that of the $\chi_2 \rightarrow \chi_1 \gamma$ process.

longer than the age of the Universe in general. Also, we should note that the net mass density of χ_1 and χ_2 does correspond to the observed DM mass density, and that it is essentially invariant throughout the evolution of the Universe in view of their negligible mass difference. We thus obtain the following relation:

$$\frac{\Omega_{\chi_2}^{ini} h^2 \exp(-\Gamma_{\chi_2} t_{cos})}{\Omega_{\chi_1}^{ini} h^2 + \Omega_{\chi_2}^{ini} h^2} \frac{\Gamma_{\chi_2}}{m} = 2.4 \times 10^{-29} \text{ s}^{-1} \text{ keV}^{-1}. \quad (4.3)$$

where $t_{cos} \simeq 4.4 \times 10^{17} \text{ s}$, and $\Omega_{\chi_i}^{ini} h^2$ denotes the mass density of χ_i ($i = 1, 2$) when it freezes out. If χ_1 and χ_2 decouple from the thermal bath in the early Universe in the same way and the relation $\Omega_{\chi_1}^{ini} h^2 = \Omega_{\chi_2}^{ini} h^2$ is satisfied, Eq. (4.3) can be reduced to

$$\Gamma_{\chi_2} t_{cos} \exp(-\Gamma_{\chi_2} t_{cos}) = \left(\frac{m_2}{100 \text{ GeV}} \right) \times 2.1 \times 10^{-4}, \quad (4.4)$$

which has two solutions of Γ_{χ_2} for each value of m_2 . Considering the range of $100 \text{ GeV} \leq m_2 \leq 1000 \text{ GeV}$, one solution is

$$\Gamma_{\chi_2} \simeq \frac{m_2}{100 \text{ GeV}} \times 4.8 \times 10^{-21} \text{ s}^{-1}, \quad (4.5)$$

and the other is numerically evaluated as

$$\Gamma_{\chi_2} \simeq 1.9 \times 10^{-17} \text{ s}^{-1} \text{ to } 1.3 \times 10^{-17} \text{ s}^{-1} \quad (4.6)$$

as m_2 varies from 100 GeV and 1 TeV. For the solution Eq. (4.6), the value of Γ_{χ_2} lies between $1.3 \times 10^{-17} \text{ s}^{-1}$ and $1.9 \times 10^{-17} \text{ s}^{-1}$ for m_2 between 1000 GeV and 100 GeV. The solution Eq. (4.5) corresponds to the case where the diminution of χ_2 up to the present is negligible, and the decay rate of χ_2 controls the flux of the 3.5-keV X-ray line. On the other hand, the solution Eq. (4.6) implies that the number of χ_2 has decreased in such a way that its number density at present gives the right flux of the 3.5-keV X-ray line. To estimate how these solutions depend on the age of the Universe, t_{cos} , we differentiate both sides of Eq. (4.3) by t_{cos} while fixing the mass of χ_2 and the observed flux of the 3.5-keV X-ray, and derive the quantity $\Delta \equiv (t_{cos}/\Gamma_{\chi_2}) |\partial \Gamma_{\chi_2} / \partial t_{cos}|$, a measure of fine-tuning. If Δ is $O(1)$ or above, this means that the solution for Γ_{χ_2} is connected with the age of the Universe, which is a miraculous coincidence that we do not expect to occur, and hence the solution is discarded. We have

$$\Delta = \frac{t_{cos}}{\Gamma_{\chi_2}} \left| \frac{\partial \Gamma_{\chi_2}}{\partial t_{cos}} \right| = \frac{t_{cos} \Gamma_{\chi_2}}{|1 - t_{cos} \Gamma_{\chi_2}|}. \quad (4.7)$$

For the solution Eq. (4.5), $\Delta \lesssim 10^{-2}$, whereas for the solution Eq. (4.6), Δ is $O(1)$. We thus dismiss the solution Eq. (4.6) for being too closely related to the age of the Universe, and only adopt the solution Eq. (4.5).

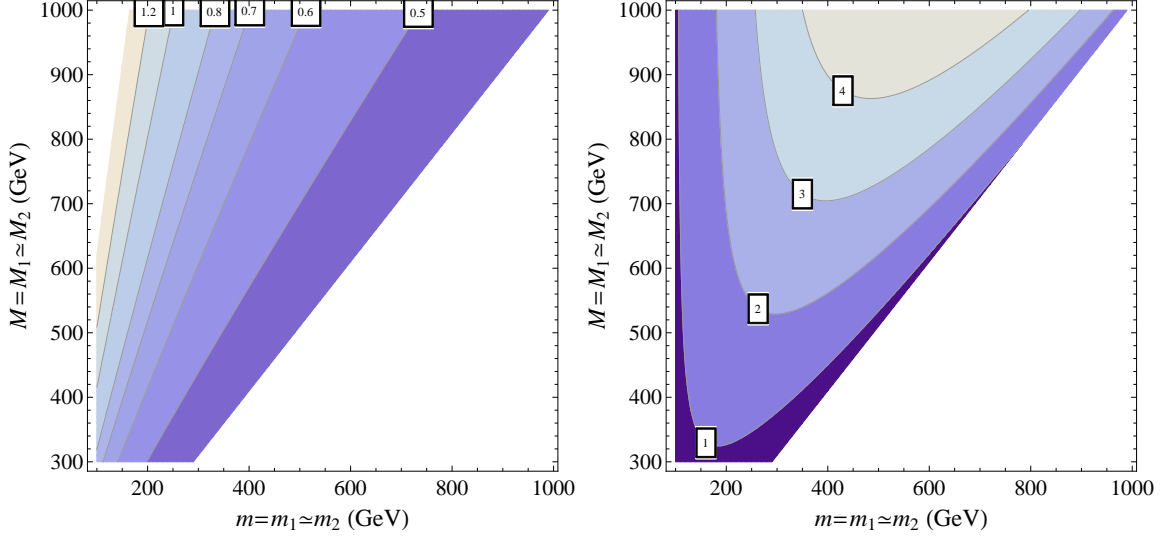


Figure 1. [Left] Contour plot of the diagonal coupling constants $\lambda = \lambda_{11} = \lambda_{22}$ that give the net thermal relic abundance of DM particles χ_1 and χ_2 that fits the Planck data, on the plane of the DM particle mass $m = m_1 \simeq m_2$ and the charged scalar mass $M = M_1 \simeq M_2$. In the upper left blank corner of the parameter space, the right DM thermal relic abundance cannot be obtained. [Right] Contour plot of ϵ in units of 10^{-8} , on the m - M plane. The off-diagonal coupling constants reproduce the correct ratio of the DM decay rate over the DM mass inferred from the flux of the 3.5-keV X-ray emission line from galaxy clusters.

5 Numerical Analysis on the Coupling Constants

From Eqs. (3.6), (3.9), (4.1) and (4.3), we can obtain information on the coupling constants λ_{ij} ($i, j = 1, 2$) for a given set of values of m_1, m_2, M_1, M_2 . In this section, we perform a numerical analysis on λ_{ij} to confirm that our model can explain both the 3.5-keV X-ray line and the DM abundance with specific values of the coupling constants. To simplify the analysis, we assume $\lambda_{11} = \lambda_{22} \equiv \lambda$ and $\lambda_{12} = -\lambda_{21} \equiv i\epsilon\lambda$, where $\lambda > 0$ and ϵ is a small real parameter. Also, we keep using the approximations that $M_1 = M_2 \equiv M$ and that $m_1 = m_2 \equiv m$ when we are allowed to neglect $m_2 - m_1$. With these simplifications, we are able to derive λ and ϵ for each set of values for m and M . In this study, we concentrate on the parameter region where $300 \text{ GeV} < M < 1 \text{ TeV}$ and $100 \text{ GeV} < m < M - 10 \text{ GeV}$.

The left plot in figure 1 is a contour plot of the diagonal coupling constants λ on the m - M plane, derived by requiring that the net thermal relic abundance of χ_1 and χ_2 fit the observed DM abundance $\Omega_{DM} h^2 = 0.1199$. The right plot in figure 1 is a contour plot of ϵ on the m - M plane, derived by requiring that the photon emission in the decay of χ_2 reproduce the observed flux of the 3.5-keV X-ray. The numbers on the contours in the right plot are displayed in units of 10^{-8} . Therefore, the off-diagonal couplings are typically smaller in size than the diagonal ones by eight orders of magnitude.

6 Phenomenology

In this section, we discuss experimental signatures of the model other than the 3.5-keV emission line.

6.1 Electric Dipole Moments

We observe from Eq. (4.1) that the decay rate of χ_2 is proportional to the square of the imaginary part of $\lambda_{11}\lambda_{21}^* + \lambda_{12}\lambda_{22}^*$. By rotating the phases of S_1, S_2 , we can always take $\lambda_{11}, \lambda_{22}$ to be real. Then the decay rate is non-zero only when $\lambda_{12} \neq \lambda_{12}^*$ or $\lambda_{21} \neq \lambda_{21}^*$ is satisfied; that is, only when the interaction in Eq. (2.1) violates CP symmetry. This is an important consequence of the Majorana nature of our DM particles: the transition magnetic dipole interaction of the Majorana DM particles Eq. (2.2), $\bar{\chi}_1 \sigma_{\mu\nu} \chi_2 F^{\mu\nu}$, which is induced at the one-loop level, flips sign under the CP transformation. Hence its effective coupling constant should be proportional to the amount of CP violation.

The CP-violating parts in Eq. (2.1) contribute to the electric dipole moment (EDM) of the SM lepton involved in the interaction. This occurs at the two-loop level. More importantly, this contribution is proportional to the mass difference between the two DM particles, $m_2 - m_1 \simeq 3.5$ keV, which can be seen as follows. Each of the two-loop diagrams contributing to the lepton EDM is proportional to either $\lambda_{11}\lambda_{21}^*\lambda_{12}^*\lambda_{22}$ or $\lambda_{12}\lambda_{22}^*\lambda_{11}^*\lambda_{21}$. By exchanging the roles of χ_1 and χ_2 in the loop of each diagram, a diagram proportional to $\lambda_{11}\lambda_{21}^*\lambda_{12}^*\lambda_{22}$ becomes one proportional to $\lambda_{12}\lambda_{22}^*\lambda_{11}^*\lambda_{21}$, and vice versa. Therefore, if the masses of χ_1 and χ_2 were the same, the sum of the two-loop lepton EDM diagrams would be proportional to $\lambda_{11}\lambda_{21}^*\lambda_{12}^*\lambda_{22} + \lambda_{12}\lambda_{22}^*\lambda_{11}^*\lambda_{21}$, which is a quantity invariant under the CP transformation, implying that the amplitude for the lepton EDM would vanish. Hence the amplitude for the lepton EDM should actually be proportional to the mass difference between χ_1 and χ_2 . In fact, the same argument applies to all orders in perturbation theory, and we conclude that the leading contribution to the lepton EDM arises at the two-loop level and is proportional to $m_2 - m_1$.

We can estimate the magnitude of the lepton EDM arising from the interaction of Eq. (2.1) by a dimensional analysis. Assuming that the charged scalar masses and the DM masses are of the same order of magnitude, denoted by M , we have

$$d_{EDM} \sim e \left(\frac{1}{16\pi^2} \right)^2 \frac{1}{M^2} (m_2 - m_1) \text{Im}(\lambda_{11}\lambda_{21}^*\lambda_{12}^*\lambda_{22}) . \quad (6.1)$$

To make an aggressive estimate, we take $\lambda_{11} = \lambda_{22} = 1$ and $\text{Im}(\lambda_{12}) = -\text{Im}(\lambda_{21}) = 5 \times 10^{-8}$ as inferred from figure 1, and assume $\text{Re}(\lambda_{12}) = -\text{Re}(\lambda_{21}) = 1$. Then, substituting $m_2 - m_1 = 3.5$ keV, we have

$$d_{EDM} \sim 3 \times 10^{-35} \left(\frac{100 \text{ GeV}}{M} \right)^2 e\text{-cm} . \quad (6.2)$$

Even when the DMs and the charged scalars couple with the SM electron, i.e., ℓ_R appearing in Eq. (2.1) is the electron, the EDM is so small for $M \simeq 100$ GeV that our model safely evades the current experimental bound.

6.2 Signatures at the LHC

In collider experiments, the most distinctive signature of our model is the existence of two charged scalars with the mass of $O(100)$ GeV that couple with DM particles and the *same* SM lepton. The most prominent process is the s-channel pair production of the charged scalars, followed by their decays into DM particles and leptons. Therefore, the signature would be a pair of opposite-sign leptons plus missing energy. In this subsection, we concentrate on the case where the charged scalars and the DMs couple with the muon for the ease of being identified particularly at hadron colliders. In our following simulations, we consider the 14-TeV LHC.

There are two strategies for testing the model at the LHC, depending on the mass degeneracy of the two charged scalars. (Although we assume in Section 5 that the charged scalar masses are equal, this is not mandatory in the model.) If the masses of the two charged scalars are different, one can confirm the existence of two charged scalar particles by reconstructing their masses using the M_{T2} variable [10]. On the other hand, even if they are degenerate, one can still gain a hint of the mass degeneracy by measuring the mass, calculating the cross section for a charged scalar pair of that mass in pp collisions, and comparing it with the measured cross section of the signal events, although these require accurate measurements of mass and cross section and precise theoretical calculations. In this subsection, we focus on the first case, and examine the possibility of testing the model at the 14-TeV LHC by simulating the charged scalar production events as well as SM background events.

Before plunging into the study on the observability of the model's signature at the LHC, we first discuss the current bounds on the model from the 8-TeV LHC experiments. The above-mentioned signature process of the charged scalar production has an event topology similar to the direct slepton (supersymmetric partner of the SM lepton) pair production followed by their prompt decays into stable neutralinos and a pair of SM leptons with opposite signs, as has been searched for by the ATLAS Collaboration [11] and the CMS Collaboration [12].

The result reported by the ATLAS Collaboration was based upon the 8-TeV data with an integrated luminosity of 20.3 fb^{-1} , and focused on the signal regions termed ‘SR- m_{T2} ’. The CMS Collaboration, on the other hand, used 19.5 fb^{-1} of data for their search analysis. Plot (a) of Fig. 8 in Ref. [11] and the bottom plot of Fig. 18 in Ref. [12] respectively give a lower bound of about 250 GeV and 190 GeV on the slepton mass at 95% confidence level.

Because of the existence of the *two* charged scalars and if the scalar masses are the same, the signal cross section in our model will double that of a supersymmetric model with only *one* flavor of $SU(2)_L$ -singlet slepton decaying into the neutralino and

the lepton. On the other hand, in our leading-order calculation with MadGraph5 [13], the production cross section of the slepton pair in pp collisions with $\sqrt{s} = 8$ TeV decreases by a factor of 2 as the slepton mass increases from 250 GeV to 300 GeV. In view of these, our model is seen to safely evade the current bounds from the LHC experiments if the masses of both charged scalars are above 300 GeV.

In the numerical study, we use MadGraph5 [13] for parton-level event generations, PYTHIA8 [14] for simulating parton showering and hadronization, and PGS4 [15] for detector simulations. We consider the following two benchmark mass spectra and coupling constants:

$$M_1 = 400 \text{ GeV} , \ M_2 = 300 \text{ GeV} , \ m_1 \simeq m_2 = 100 \text{ GeV} , \ \lambda_{11} = \lambda_{22} = 0.8 ; \quad (6.3)$$

$$M_1 = 500 \text{ GeV} , \ M_2 = 300 \text{ GeV} , \ m_1 \simeq m_2 = 100 \text{ GeV} , \ \lambda_{11} = \lambda_{22} = 1.0 . \quad (6.4)$$

We generate parton-level events for the following signal processes for $i = 1, 2$, where j denotes any parton:

$$\begin{aligned} p p &\rightarrow S_i S_i^\dagger, \quad S_i \rightarrow \chi_i \mu^+, \quad S_i^\dagger \rightarrow \chi_i \mu^-, \\ p p &\rightarrow S_i S_i^\dagger j, \quad S_i \rightarrow \chi_i \mu^+, \quad S_i^\dagger \rightarrow \chi_i \mu^-, \quad (i = 1, 2). \end{aligned} \quad (6.5)$$

Values of the coupling constants affect collider signatures by changing the widths of the charged scalars, yet such effects are negligible. The 0-jet and 1-jet events are matched after parton showering by the MLM matching scheme [16], and the showered and hadronized events are processed for the detector simulation. Jets are reconstructed by the anti- k_T jet clustering algorithm [17] with $\Delta R = 0.4$. We include both the 0-jet and 1-jet events to take into account the effect of an initial state radiation jet(s), the mismeasurement of which causes the uncertainty of missing transverse momentum.

The dominant sources of SM background are diboson W^+W^- , ZZ and $Z\gamma$ production processes. We therefore generate parton-level events for the following background processes, where j denotes any parton,

$$\begin{aligned} p p &\rightarrow W^+ W^-, \quad W^+ \rightarrow \mu^+ \nu_\mu, \quad W^- \rightarrow \mu^- \bar{\nu}_\mu, \\ p p &\rightarrow W^+ W^- j, \quad W^+ \rightarrow \mu^+ \nu_\mu, \quad W^- \rightarrow \mu^- \bar{\nu}_\mu, \\ p p &\rightarrow Z Z^*/\gamma(\rightarrow \mu^+ \mu^-), \quad Z \rightarrow \nu \bar{\nu}, \\ p p &\rightarrow Z Z^*/\gamma(\rightarrow \mu^+ \mu^-) j, \quad Z \rightarrow \nu \bar{\nu}, \end{aligned} \quad (6.6)$$

and the generated events are processed in the same way as the signal events. Since we will impose a selection cut of $m(\mu^+, \mu^-) > 150$ GeV, we only generate those events where a $\mu^+\mu^-$ pair is produced through an off-shell Z boson or a photon.

We impose the following kinetic cuts on the events after detector simulation:

- (a) There should be two opposite-sign muons whose pseudo-rapidity and transverse momentum satisfy $|\eta_\mu| < 2.4$ and $p_T^\mu > 25$ GeV.

- (b) The missing transverse momentum should satisfy $\cancel{p}_T > 200$ GeV.
- (c) The invariant mass of the muons should satisfy $m(\mu^+, \mu^-) > 150$ GeV.
- (d) The muons should be separated from any jet by the distance of $\Delta R(\vec{p}_\mu, \vec{p}_j) > 0.4$.

We evaluate the M_{T2} variable, defined as

$$M_{T2}^2 = \min_{\vec{p}_1 + \vec{p}_2 = \vec{\cancel{p}}_T} [\max\{M_T(\vec{p}_{\mu^+}, \vec{p}_1), M_T(\vec{p}_{\mu^-}, \vec{p}_2)\}], \quad (6.7)$$

for each event and plot its distribution for both the signal and background processes in figure 2.

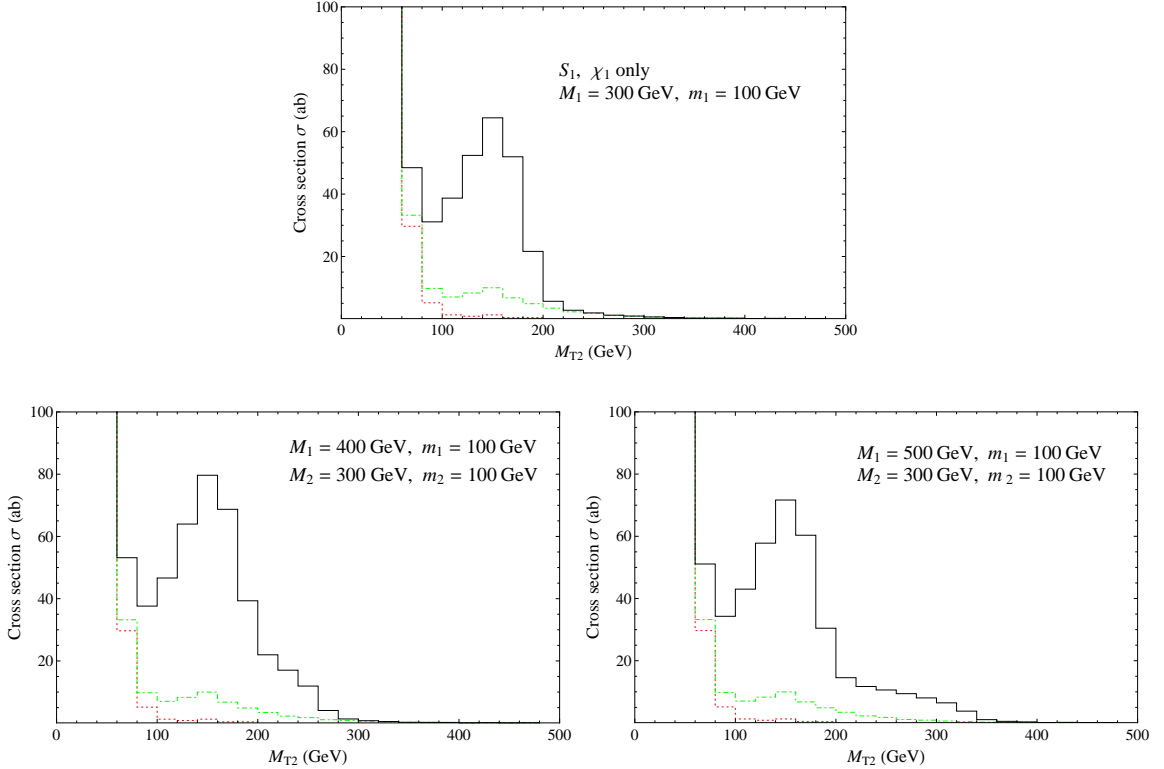


Figure 2. Each plot shows the M_{T2} distribution for the SM W^+W^- production process (red dotted line), that plus the SM ZZ/γ production processes (green dot-dashed line), and those plus the signal $S_i S_i^\dagger$ ($i = 1, 2$) production processes followed by the S_i decay into a muon and a DM particle χ_i , at the 14-TeV LHC. The simulation is done at the detector level, after imposing the selection cuts (a), (b), and (c) defined in the text. The upper plot corresponds to the case where there exist only S_1 and χ_1 particles whose masses are respectively $M_1 = 300$ GeV and $m_1 = 100$ GeV, the lower left plot to the benchmark mass spectrum in Eq. (6.3), and the lower right plot to the benchmark mass spectrum in Eq. (6.4). The vertical bars in the histograms are in units of ab per 20-GeV bin.

In figure 2, we observe a difference in the tails of the M_{T2} distributions for the case where there is only one set of charged scalar and DM particle and the cases

where there are two charged scalars of different masses each of which couples with a different DM particle. Compared to the signals of our benchmark mass spectra in Eqs. (6.3, 6.4), the SM backgrounds are well suppressed with the cuts (a), (b), and (c). We therefore conclude that, with $\sim 1 \text{ ab}^{-1}$ of data at the 14-TeV LHC, there is a good chance to confirm the existence of two charged scalar-DM pairs, if the charged scalar masses are separated by $O(100)$ GeV and both of them are below about 500 GeV.

7 Summary

We have proposed and studied a model where the unidentified 3.5-keV X-ray emission line from galaxy clusters is explained in terms of the decay of a WIMP DM particle into another WIMP DM particle and a photon. We have argued that the simplest model is the one that contains two spin-1/2 Majorana DM particles with the mass difference of 3.5 keV and coupling with two charged scalars of $O(100)$ GeV mass and a SM matter fermion(s). Each DM particle couples dominantly with a distinct charged scalar and the same SM matter fermion through an $O(0.1)$ coupling constant, which is responsible for the thermalization of the DM in the early Universe and realizes the WIMP DM scenario. On the other hand, each DM particle also couples with the other charged scalar through a tiny coupling constant of order 10^{-8} , which induces a dipole transition coupling between the two DM species at one-loop level, thereby giving rise to the decay of the heavier DM into the lighter one and the photon.

As prominent phenomenological signatures of the model, we have discussed the contribution of the new particles to the EDM of the SM matter, and the collider signatures of the charged scalars at the 14-TeV LHC. We emphasize that, since the dipole transition operator of the Majorana fermions violates CP symmetry, one can infer the CP-violating part of the charged scalar-DM-SM matter fermion couplings from the DM decay rate, which is directly connected with the flux of the 3.5-keV emission line. We have discovered that the induced lepton EDM is so tiny that it safely evades the current experimental bound even when the SM matter is the electron. Also, we have studied the signatures of the model at the 14-TeV LHC, paying particular attention to whether one can confirm the existence of the two-component charged scalars when their masses are separate. By observing the shape of the tail in the M_{T2} distribution, it is possible to distinguish the cases where there is only one set of charged scalar and DM particle that couple with the SM muon and where there are two charged scalar-DM sets, provided the mass difference is of the order of 100 GeV and the charged scalar masses are below about 500 GeV.

Note Added: While this work was being written up, we noticed a similar work by Geng et. al. [18]. However, our model is different from theirs in the number of charged scalars and the associated interactions. Therefore, we have different collider signatures for the new particles. In addition, unlike their model, ours does not introduce new sources for lepton flavor violating processes. Neither do we have the transition electric dipole coupling of two Majorana DM particles at the one-loop level, and only the transition magnetic dipole coupling appears in our model.

Acknowledgments

The authors would like to thank K. Yagyu for participating in discussions during the early stage of this project. C.-W. C. thanks the hospitality of the KITP at Santa Barbara where last part of this work was being finished. This research was supported in part by the National Science Council of R.O.C. under Grant Nos. NSC-100-2628-M-008-003-MY4 and NSC-102-2811-M-008-019 and in part by the National Science Foundation under Grant No. NSF PHY11-25915.

References

- [1] E. Bulbul, M. Markevitch, A. Foster, R. K. Smith, M. Loewenstein and S. W. Randall, *Astrophys. J.* **789**, 13 (2014) [arXiv:1402.2301 [astro-ph.CO]].
- [2] A. Boyarsky, O. Ruchayskiy, D. Iakubovskiy and J. Franse, arXiv:1402.4119 [astro-ph.CO].
- [3] H. Ishida, K. S. Jeong and F. Takahashi, *Phys. Lett. B* **732**, 196 (2014) [arXiv:1402.5837 [hep-ph]]; D. P. Finkbeiner and N. Weiner, arXiv:1402.6671 [hep-ph]; T. Higaki, K. S. Jeong and F. Takahashi, *Phys. Lett. B* **733**, 25 (2014) [arXiv:1402.6965 [hep-ph]]; J. Jaeckel, J. Redondo and A. Ringwald, *Phys. Rev. D* **89**, 103511 (2014) [arXiv:1402.7335 [hep-ph]]; H. M. Lee, S. C. Park and W. -I. Park, arXiv:1403.0865 [astro-ph.CO]; K. N. Abazajian, *Phys. Rev. Lett.* **112**, 161303 (2014) [arXiv:1403.0954 [astro-ph.CO]]; C. El Aisati, T. Hambye and T. Scarna, arXiv:1403.1280 [hep-ph]; K. Hamaguchi, M. Ibe, T. T. Yanagida and N. Yokozaki, arXiv:1403.1398 [hep-ph]; J. -C. Park, S. C. Park and K. Kong, *Phys. Lett. B* **733**, 217 (2014) [arXiv:1403.1536 [hep-ph]]; M. T. Frandsen, F. Sannino, I. M. Shoemaker and O. Svendsen, *JCAP* **1405**, 033 (2014) [arXiv:1403.1570 [hep-ph]]; S. Baek and H. Okada, arXiv:1403.1710 [hep-ph]; K. Nakayama, F. Takahashi and T. T. Yanagida, arXiv:1403.1733 [hep-ph]; K. -Y. Choi and O. Seto, *Phys. Lett. B* **735**, 92 (2014) [arXiv:1403.1782 [hep-ph]]; M. Cicoli, J. P. Conlon, M. C. D. Marsh and M. Rummel, arXiv:1403.2370 [hep-ph]; F. Bezrukov and D. Gorbunov, arXiv:1403.4638 [hep-ph]; C. Kolda and J. Unwin, arXiv:1403.5580 [hep-ph]; R. Allahverdi, B. Dutta and Y. Gao, arXiv:1403.5717 [hep-ph]; N. -E. Bomark and L. Roszkowski, arXiv:1403.6503 [hep-ph]; S. P. Liew,

- JCAP **1405**, 044 (2014) [arXiv:1403.6621 [hep-ph]; Z. Kang, P. Ko, T. Li and Y. Liu, arXiv:1403.7742 [hep-ph]; S. V. Demidov and D. S. Gorbunov, arXiv:1404.1339 [hep-ph]; F. S. Queiroz and K. Sinha, Phys. Lett. B **735**, 69 (2014) [arXiv:1404.1400 [hep-ph]]; E. Dudas, L. Heurtier and Y. Mambrini, arXiv:1404.1927 [hep-ph]; K. S. Babu and R. N. Mohapatra, Phys. Rev. D **89**, 115011 (2014) [arXiv:1404.2220 [hep-ph]]; K. P. Modak, arXiv:1404.3676 [hep-ph]; J. M. Cline, Y. Farzan, Z. Liu, G. D. Moore and W. Xue, arXiv:1404.3729 [hep-ph]; H. Okada and T. Toma, arXiv:1404.4795 [hep-ph]; H. M. Lee, arXiv:1404.5446 [hep-ph]; D. J. Robinson and Y. Tsai, arXiv:1404.7118 [hep-ph]; J. P. Conlon and F. V. Day, arXiv:1404.7741 [hep-ph]; S. Baek, P. Ko and W. -I. Park, arXiv:1405.3730 [hep-ph]; K. Nakayama, F. Takahashi and T. T. Yanagida, arXiv:1405.4670 [hep-ph]; S. Chakraborty, D. K. Ghosh and S. Roy, arXiv:1405.6967 [hep-ph]; N. Chen, Z. Liu and P. Nath, arXiv:1406.0687 [hep-ph]; J. P. Conlon and A. J. Powell, arXiv:1406.5518 [hep-ph]; H. Ishida and H. Okada, arXiv:1406.5808 [hep-ph].
- [4] E. Masso, S. Mohanty and S. Rao, Phys. Rev. D **80**, 036009 (2009) [arXiv:0906.1979 [hep-ph]].
- [5] Y. Gao, C. M. Ho and R. J. Scherrer, Phys. Rev. D **89**, 045006 (2014) [arXiv:1311.5630 [hep-ph]].
- [6] N. Okada and T. Yamada, JHEP **1310**, 017 (2013) [arXiv:1304.2962 [hep-ph]].
- [7] See, e.g., E. W. Kolb, and M. S. Turner, *The Early Universe* (Addison-Wesley).
- [8] J. Edsjo and P. Gondolo, Phys. Rev. D **56**, 1879 (1997) [hep-ph/9704361].
- [9] P. A. R. Ade *et al.* (Planck Collaboration) [arXiv:1303.5076].
- [10] C. G. Lester and D. J. Summers, Phys. Lett. B **463**, 99 (1999) [hep-ph/9906349].
- [11] ATLAS collaboration, JHEP **05**, 071 (2014) [arXiv:1403.5294 [hep-ex]].
- [12] CMS collaboration, arXiv:1405.7570 [hep-ex].
- [13] J. Alwall *et al.*, JHEP **0709**, 028 (2007) [arXiv:0706.2334[hep-ph]]; J. Alwall, M. Herquet, F. Maltoni, O. Mattelaer and T. Stelzer, JHEP **1106**, 128 (2011) [arXiv:1106.0522[hep-ph]].
- [14] T. Sjostrand, S. Mrenna and P. Z. Skands, JHEP **0605**, 026 (2006) [arXiv:hep-ph/0603175].
- [15] J. Conway *et al.*, PGS (Pretty Good Simulation) (2009), <http://physics.ucdavis.edu/conway/research/software/pgs/pgs4-general.htm>.
- [16] M. L. Mangano, M. Moretti and R. Pittau, Nucl. Phys. B **632**, 343 (2002) [arXiv:hep-ph/0108069]; M. L. Mangano, M. Moretti, F. Piccinini and M. Treccani, JHEP **0701**, 013 (2007) [arXiv:hep-ph/0611129].
- [17] M. Cacciari, G. P. Salam and G. Soyez, JHEP **0804**, 063 (2008) [arXiv:0802.1189 [hep-ph]].
- [18] C. -Q. Geng, D. Huang and L. -H. Tsai, arXiv:1406.6481 [hep-ph].